

# Persistence Problem in Two-Dimensional Fluid Turbulence

Prasad Perlekar,<sup>1,\*</sup> Samriddhi Sankar Ray,<sup>2,3,†</sup> Dhrubaditya Mitra,<sup>4,‡</sup> and Rahul Pandit<sup>2,§</sup>

<sup>1</sup> *Department of Physics and Department of Mathematics and Computer Science. Eindhoven University of Technology, P.O. Box 513, 5600 MB Eindhoven, The Netherlands*

<sup>2</sup> *Centre for Condensed Matter Theory, Department of Physics, Indian Institute of Science, Bangalore 560012, India.*

<sup>3</sup> *Laboratoire Cassiopée, Observatoire de la Côte d'Azur, UNS, CNRS, BP 4229, 06304 Nice Cedex 4, France.*

<sup>4</sup> *NORDITA, Roslagstullsbacken 23, SE-10691 Stockholm, Sweden*

We present a natural framework for studying the persistence problem in two-dimensional fluid turbulence by using the Okubo-Weiss parameter  $\Lambda$  to distinguish between vortical and extensional regions. We then use a direct numerical simulation (DNS) of the two-dimensional, incompressible Navier-Stokes equation with Ekman friction to study probability distribution functions (PDFs) of the persistence times of vortical and extensional regions by employing both Eulerian and Lagrangian measurements. We find that, in the Eulerian case, the persistence-time PDFs have exponential tails; by contrast, this PDF for Lagrangian particles, in vortical regions, has a power-law tail with an exponent  $\theta = 2.9 \pm 0.2$ .

PACS numbers: 47.27.-i, 05.40.-a

Keywords: turbulence, statistical mechanics, persistence

The persistence problem, which is of central importance in nonequilibrium statistical mechanics [1], is defined as follows: For a fluctuating field  $\phi$ , the persistence-time probability distribution function (PDF)  $P^\phi(\tau)$  yields the probability that the sign of  $\phi$  at a point in space does not change up to a time  $\tau$ . Theoretical, experimental, and numerical studies of a variety of systems, ranging from reaction-diffusion systems to granular media, have shown that  $P^\phi(\tau) \sim \tau^{-\theta}$  as  $\tau \rightarrow \infty$ , where  $\theta$  is the *persistence exponent*. This nontrivial exponent cannot be obtained from dimensional arguments; it can be calculated analytically only for a few models [2]; for most models it has to be obtained numerically. We propose a natural way of defining the persistence problem in two-dimensional turbulence. We then show how to obtain the persistence exponent for this case.

Turbulent flows in two-dimensional fluid films display vortical points and strain-dominated or extensional points. We show how to examine the *persistence* of such points in time by direct numerical simulations (DNSs) of the forced, two-dimensional, incompressible Navier-Stokes equation. Our study has been designed with thin-fluid-film experiments in mind [3, 4] so we account for an air-drag-induced Ekman friction and we drive the fluid by using a Kolmogorov forcing. We demonstrate that the Okubo-Weiss parameter [5, 6]  $\Lambda$ , whose sign at a given point determines whether the flow there is vortical or extensional, provides us with a natural way of studying such persistence.

It is important to distinguish the following types of persistence times: (A) In the Eulerian framework we consider a point  $(x, y)$  and, by following the time evolution of  $\Lambda$ , determine the time  $\tau$  for which the flow at this point remains vortical (extensional) if the flow at this point became vortical (extensional) at some earlier time; (B)

in the Lagrangian framework we consider how long a Lagrangian particle resides in a vortical (extensional) region if this particle entered that vortical (extensional) region at an earlier time. For all these cases we obtain PDFs of the persistence or residence times that we denote generically by  $\tau$ . We find, in the Eulerian framework, that the PDFs of  $\tau$  show exponential tails in both vortical and extensional regions. In the Lagrangian framework the PDF of the residence time of the particle in extensional regions also shows an exponential tail; the analogous PDF for vortical regions shows a *power-law tail*. The persistence exponent that characterizes this power law is independent of parameters such as the Reynolds number, the characteristic scale of the forcing, and the coefficient of Ekman friction, at least at the level of our numerical studies.

We perform a direct numerical simulation (DNS) of the incompressible, two-dimensional, Navier-Stokes equation

$$\partial_t \omega - J(\psi, \omega) = \nu \nabla^2 \omega + f_\omega - \mu \omega, \quad (1)$$

with periodic boundary conditions, by using a pseudospectral method [7] with  $N^2$  collocation points and the 2/3 dealiasing rule. Here  $\psi$  is the stream function,  $\omega$  the vorticity,  $J(\psi, \omega) \equiv (\partial_x \psi)(\partial_y \omega) - (\partial_x \omega)(\partial_y \psi)$ ,  $\nu$  the kinematic viscosity, and  $\mu$  the coefficient of Ekman friction. At the point  $(x, y)$  the velocity  $\mathbf{u} \equiv (-\partial_y \psi, \partial_x \psi)$  and the vorticity  $\omega = \nabla^2 \psi$ ; the external deterministic force  $f_\omega(x, y) = -F_0 k_{\text{inj}} \cos(k_{\text{inj}} x)$ , where  $F_0$  is an amplitude and  $k_{\text{inj}}$  the energy-injection scale in Fourier space. The injected energy displays an inverse cascade to small  $k$ . Ekman friction removes energy from all Fourier modes; in particular, it removes energy from small- $k$  Fourier modes in such a way that the system reaches a nonequilibrium statistically steady state. We evolve Eq. 1 in time by a second-order, exponential Runge-Kutta method [8]. In

all our simulations we wait for a time  $T_{\text{tran}}$  [see the caption of Table (I)] to allow transients to die out so that our system reaches a statistically steady state. Figure (1) shows a typical pseudocolor plot of  $\psi$  in such a state.

To calculate Lagrangian quantities we track  $N_p$  particles. The evolution equation for a Lagrangian particle is  $\frac{d}{dt}\mathbf{x}_L(t) = \mathbf{u}(\mathbf{x}_L, t)$ , where  $\mathbf{x}_L(t)$  is the position of a Lagrangian particle at time  $t$ ;  $\mathbf{u}(\mathbf{x}_L, t)$ , the velocity at the Lagrangian particle position, is evaluated from the Eulerian velocity field  $\mathbf{u}(\mathbf{x}, t)$  by using a bilinear-interpolation scheme [9]. The evolution equation of the particles is solved by a second-order, Runge-Kutta method [9]. Initially all the particles are seeded randomly into the flow. A typical Lagrangian-particle track superimposed on a representative pseudocolor plot of  $\psi$  is shown in Fig. (1). The list of parameters used in our simulations is given in Table (I).

From the velocity-gradient tensor  $\mathcal{A}$ , with components  $A_{ij} \equiv \partial_i u_j$ , we obtain the Okubo-Weiss parameter  $\Lambda$ , the discriminant of the characteristic equation for  $\mathcal{A}$ . If  $\Lambda$  is positive (negative) then the flow is vortical (extensional) [5]. In an incompressible flow in two dimensions  $\Lambda = \det \mathcal{A}$ ; and the PDF of  $\Lambda$  has been shown [4] to be asymmetrical about  $\Lambda = 0$  (vortical regions are more likely to occur than strain-dominated ones). For the Eulerian case, we monitor the time evolution of  $\Lambda$  at  $N_p$  randomly chosen points that are fixed in the simulation domain. In our Lagrangian study, we begin with the values of  $\Lambda$  on the spatial grid that we use for our Eulerian DNS; bilinear interpolation then yields  $\Lambda$  at the positions of Lagrangian particles, which can be at points that do not lie on this grid; we can thus monitor the evolution of  $\Lambda$  along Lagrangian-particle trajectories.

We denote the persistence-time PDFs by  $P$  and the associated cumulative PDFs by  $Q$ ; the subscripts  $E$  and  $L$  on these PDFs signify Eulerian and Lagrangian frames, respectively; and the superscripts  $+$  or  $-$  distinguish PDFs from vortical points from those from extensional ones. To find out the persistence-time PDF  $P_E^+(\tau)$  [resp.,  $P_E^-(\tau)$ ] we analyse the time-series of  $\Lambda$  obtained from each of the  $N_p$  Eulerian points and construct the PDF of the time-intervals  $\tau$  over which  $\Lambda$  remains positive (resp., negative). The same method applied to the time series of  $\Lambda$ , obtained from each of the  $N_p$  Lagrangian particles, yields  $P_L^+(\tau)$  [resp.,  $P_L^-(\tau)$ ].

We use the rank-order method [10] to calculate cumulative PDFs because they are free from binning errors. We show representative plots of the cumulative PDFs  $Q_E^+$  (red crosses),  $Q_E^-$  (black open circles), and  $Q_L^-$  (magenta full circles) in Fig. (2a); the dashed lines indicate exponential fits to these cumulative PDFs. From these and similar fits we conclude that the PDFs  $P_E^+$ ,  $P_E^-$ , and  $P_L^-$  have exponentially decaying tails, for all the runs, from which we can extract characteristic time scales. In particular, from the Eulerian PDFs we obtain the times  $T_E^+$  and  $T_E^-$ , for vortical and strain-

dominated regions, respectively, which are defined as follows:  $P_E^+(\tau) \sim \exp(-\tau/T_E^+)$  and  $P_E^-(\tau) \sim \exp(-\tau/T_E^-)$  as  $\tau \rightarrow \infty$  [see Table (I)]. The Lagrangian PDF  $P_L^-$  also has an exponentially decaying tails from which we obtain the characteristic time  $T_L^-$  [see Table (I)].

The persistence-time PDF  $P_L^+$  and the associated cumulative PDF  $Q_L^+$  of a Lagrangian particle in a vortical region is very different from those discussed above: the tails of  $P_L^+$  and  $Q_L^+$  have power-law, and not exponential, forms; we show this in Fig. (2b) via a representative plot  $Q_L^+$  for the run R4. Thus, as in nonequilibrium statistical mechanics [1], we can define the persistence exponent  $\theta$  via  $P_L^+ \sim \tau^{-\theta}$ . Our run R4 has the largest value of  $Re_\lambda$  amongst the runs R1 – 4 [Table (I)] and, therefore, is best suited for estimating  $\theta$  from plots such as the one in Fig. (2b). We obtain the exponent  $(-\theta + 1)$  by fitting a power-law to the tail of the cumulative PDF  $Q_L^+$ . To find the best estimate for  $(-\theta + 1)$  we evaluate the local slope  $\chi = d \log_{10} Q_L^+(\tau) / d \log_{10}(\tau)$  in the region shown in the inset of Fig. (2b). Our estimate for  $(-\theta + 1)$  is the mean value of  $\chi$  over the region indicated in the inset; the standard deviation of  $\chi$  yields the error; finally we obtain  $\theta = 2.9 \pm 0.2$ . Our other runs R1 – 3 yield smaller scaling ranges than the one in Fig. (2b) and, therefore, yield values for  $\theta$  with larger error bars; but these values are consistent with our estimate for  $\theta$  from run R4. We also find that the persistence exponent  $\theta$  does not depend on the parameters  $\mu$ ,  $F_0$ , and  $k_{\text{inj}}$  (within error-bars) in the range of parameters accessible in our simulations. Based on this evidence we conjecture that  $\theta$  is a new universal exponent that characterizes two-dimensional, Navier–Stokes turbulence. A conclusive proof of this conjecture must await future studies.

The exponent  $\theta > 1$ , so we can obtain the average lifetime  $T_{\text{mean}}^+$  of a particle in a vortical region from  $P_L^+$ ; Another estimate of the lifetime of vortices in the Lagrangian frame is given by the time scale  $T_{\text{cf}}$ , which is the cutoff scale of the power-law decay of tail of  $P_L^+$ , [Table (I)].

In most persistence problems in nonequilibrium statistical mechanics the power-law tail for the persistence-time PDF appears in the following way: Typically we consider the persistence-time PDF of  $\phi$  that comes from a Gaussian, but *non-stationary*, process; a transformation to logarithmic time  $s$  transforms such a process to a Gaussian stationary process (GSP)  $X(s)$ ; if, in addition, the GSP is also Markovian, i.e., the autocorrelation function of the GSP,  $f(t) = \langle X(s)X(s+t) \rangle_s$ , is an exponential function of  $t$ , then the persistence-time PDF of the GSP can be shown to have an exponential tail [1]. If we now transform back from logarithmic to linear time, the exponential tail is transformed to a power-law tail. Furthermore, for a GSP for which the autocorrelation function  $f(t)$  decays faster than  $1/t$  for large  $t$ , the persistence-time PDF  $P(t) \sim \exp(-\gamma t)$ , where  $\gamma$  is a constant [1].

In the two-dimensional, fluid-turbulence problem that

we study here, we have checked numerically that  $\Lambda$  is a stationary process; hence we do not need to transform to logarithmic time. We have calculated two types of autocorrelation functions for  $\Lambda$  (we denote these generically by  $C_\Lambda(t)$  in Fig. (2c)): (a) For the first we evaluate  $\langle \Lambda(0)\Lambda(t) \rangle$  over the track of a Lagrangian particle; this is shown by blue open circles in Fig. (2c); (b) for the second we evaluate  $\langle \Lambda(0)\Lambda(t) \rangle$  at a given point on our Eulerian grid; this is shown by red full circles in Fig. (2c); here  $\langle \cdot \rangle$  denotes averages over different origins of time and also over  $N_p$  different Lagrangian particles, for case (a), or over  $N_p$  different Eulerian positions, for case (b). As we show in the inset of Fig. (2c) for both these cases,  $C_\Lambda(t)$  is approximated well by the function  $\exp[-(t/T_\Lambda)^2]$ , over the range  $10^{-4} < (t/T_\eta) < 10^{-1}$ ; this decay is clearly faster than  $1/t$  for large  $t$ . Here  $T_\Lambda$ , the characteristic decay time, is slightly larger in the Lagrangian case than in the Eulerian one; however, in both these cases  $T_\Lambda \simeq T_\eta$ . Plots of  $C_\Lambda$  from our other runs R1 – 3 are similar to the one in Fig. (2c) from run R4. Note that, in the problem we study, the persistence-time PDF is not constrained to have an exponential tail because  $\Lambda$ , although stationary, is not a Gaussian process.

We have presented a natural framework for studying the persistence problem in two-dimensional fluid turbulence. The most important result of our study is that the persistence-time PDFs for vortical points show qualitatively different behaviors in the Eulerian and Lagrangian cases: In vortical regions, for the Eulerian case, this PDF displays an exponential decay; in contrast, for the Lagrangian case it shows a power-law tail. Qualitatively such nontrivial behavior appears because a passive particle can be trapped for quite some time in a vortical region [11]. Furthermore, we provide a way of measuring the lifetime of a vortex precisely. In the Eulerian frame the characteristic lifetime of a vortex is the time scale  $T_E^+$  that follows from the exponential form  $P_E^+(\tau) \sim \exp(-\tau/T_E^+)$ . However, in the Lagrangian frame the persistence-time PDF for vortical points shows a power-law decay with a persistence-time exponent  $\theta = 2.9 \pm 0.2$ . Hence there is no single time scale which describes the time spent by passive particles in vortical points; but, as we have mentioned above, an average residence time can be defined because  $\theta > 1$ .

The PDF of residence times of passive tracers in vortical regions  $P_L^+$  is of great fundamental and engineering importance. Earlier studies [12, 13] have attempted to measure this PDF; however, their methods of obtaining it are not as precise as the one we present here: the Okubo-Weiss parameter  $\Lambda$ , which we employ, helps us to distinguish clearly between vortical and extensional regions in the two-dimensional flows we consider. The natural way of generalizing our study to its three-dimensional counterpart is to replace the Okubo-Weiss parameter by  $QR$  plots [14] and then to study the PDFs of residence times of Lagrangian particles in each quadrant of the  $QR$

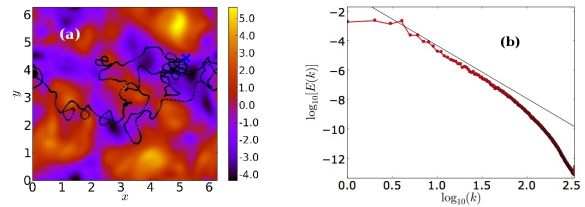


FIG. 1: (Color online) (a) A pseudocolor plot of the stream function  $\psi$ , at a representative time in the statistically steady state, with a representative Lagrangian particle track (blue squares) superimposed on it from our run R2. The symbol o indicates the beginning of the trajectory and the  $\times$  sign marks its end. For an animated version see the movie file at <http://www.youtube.com/watch?v=ANDUNDHYgzk>; (b) log-log (base 10) plot of the energy spectrum for our run R4 (line with red dots); the black line with a slope  $-3.6$  is shown for reference.

plot; here  $Q = -\frac{1}{2}\text{tr}(\mathcal{A}^2)$  and  $R = -\frac{1}{3}\text{tr}(\mathcal{A}^3)$  where  $\mathcal{A}$  is the velocity gradient matrix. It remains to be seen whether the tails of such PDFs have power-law tails in three-dimensional turbulence; such a study lies beyond the scope of this paper. From the point of view of the general theory of persistence problems, the time-series of  $\Lambda$  in the Lagrangian frame provides a particularly interesting example. The persistence-time PDF has a power-law behavior for positive  $\Lambda$  but an exponential tail for negative  $\Lambda$ . A similar, but less dramatic, example of such asymmetry has been observed for the case of growing interfaces whose height  $h$  obeys the Kardar-Parisi-Zhang (KPZ) equation [15]. For this KPZ case, the persistence-time PDF shows power-law tails, but with different persistence-time exponents for positive and negative  $h$ . We hope our study will stimulate new experimental investigations of persistence-time PDFs in two-dimensional fluid turbulence and also studies of such PDFs for other non-Gaussian, stationary processes.

We thank S. Krishnamurthy and D. Sanyal for discussions, the European Research Council under the AstroDyn Research Project No. 227952, CSIR, UGC, and DST (India) for support and SERC (IISc) for computational resources. PP and RP are members of the International Collaboration for Turbulence Research; RP, PP, and SSR acknowledge support from the COST Action MP0806.

\* Electronic address: p.perlekar@tue.nl

† Electronic address: samriddhisankarray@gmail.com

‡ Electronic address: dhruba.mitra@gmail.com

§ Electronic address: rahul@physics.iisc.ernet.in; also at Jawaharlal Nehru Centre For Advanced Scientific Research, Jakkur, Bangalore, India.

- [1] See, e.g., S.N. Majumdar, Curr. Sci. **77**, 370 (1999) and references therein.
- [2] S. Majumdar, C. Sire, A. Bray, and S. Cornell, Phys.

Run	$N$	$\nu$	$\mu$	$F_0$	$k_{\text{inj}}$	$l_d$	$\lambda$	$Re_\lambda$	$T_{\text{eddy}}$	$T_\eta$	$T_E^-$	$T_L^-$	$T_E^+$	$T_{\text{mean}}^+$	$T_{\text{inj}}$	$T_{\text{cf}}$
R1	512	0.016	0.1	45	10	$2.3 \times 10^{-2}$	0.2	59	0.1	$3.4 \times 10^{-2}$	$0.3 \pm 0.04$	$0.12 \pm 0.02$	$0.21 \pm 0.05$	$2.8 \times 10^{-2}$	0.3	0.9
R2	512	0.016	0.45	45	10	$2.1 \times 10^{-2}$	0.1	27	0.1	$2.7 \times 10^{-2}$	$0.4 \pm 0.05$	$0.17 \pm 0.02$	$0.24 \pm 0.03$	$4.2 \times 10^{-2}$	0.2	0.8
R3	1024	$10^{-5}$	0.01	0.005	10	$4.3 \times 10^{-3}$	0.1	827	11	1.9	$19 \pm 3$	$10 \pm 2$	$13 \pm 2$	1.8	19.9	76
R4	1024	$10^{-5}$	0.01	0.005	4	$5.4 \times 10^{-3}$	0.2	1319	7	2.9	$31 \pm 5$	$15 \pm 2$	$25 \pm 4$	2.5	30.2	81

TABLE I: Parameters for our runs R1–4:  $N$  is the number of grid points along each direction,  $N_p = 1000$  is the number of Lagrangian particles and Eulerian positions (at which we monitor  $\Lambda$ ),  $\nu$  the kinematic viscosity,  $\mu$  the Ekman friction,  $F_0$  the forcing amplitude,  $k_{\text{inj}}$  the forcing wavenumber,  $l_d \equiv (\nu^3/\varepsilon)^{1/4}$  the dissipation scale,  $\lambda \equiv \sqrt{\nu E/\varepsilon}$  the Taylor microscale,  $Re_\lambda \equiv u_{\text{rms}}\lambda/\nu$  the Taylor-microscale Reynolds number,  $T_{\text{eddy}} \equiv [\pi \sum_k (E(k)/k)/(2u_{\text{rms}}^2)]$  the eddy-turn-over time, and  $T_\eta \equiv \sqrt{\nu/\varepsilon}$  the Kolmogorov time scale. The time scales  $T_E^-$ ,  $T_L^-$  and  $T_E^+$  are obtained from exponential fits to the tails of the cumulative PDFs  $Q_E^-$ ,  $Q_L^-$  and  $Q_E^+$ , respectively, as shown in Fig (2a).  $T_{\text{mean}}^+$  is the average time spent by a Lagrangian particle in a vortical region,  $T_{\text{inj}} \equiv (l_{\text{inj}}^2/E_{\text{inj}})^{1/3}$  is the energy-injection time scale, where  $E_{\text{inj}} = \langle \mathbf{f}_u \cdot \mathbf{u} \rangle$ , ( $\mathbf{f}_u = \nabla \times \mathbf{f}_u$ ), is the energy-injection rate and  $l_{\text{inj}} = 2\pi/k_{\text{inj}}$  is the energy-injection length scale.  $T_{\text{cf}}$  is the large-time cutoff of the scaling range of  $Q_L^+$  as shown in Fig. 2b. We do not use data from the initial period of duration  $T_{\text{tran}} = 100T_{\text{eddy}}$ ; this removes the effects of transients. We use a square simulation domain with side  $L = 2\pi$  and grid spacing  $\delta_x = L/N$ .

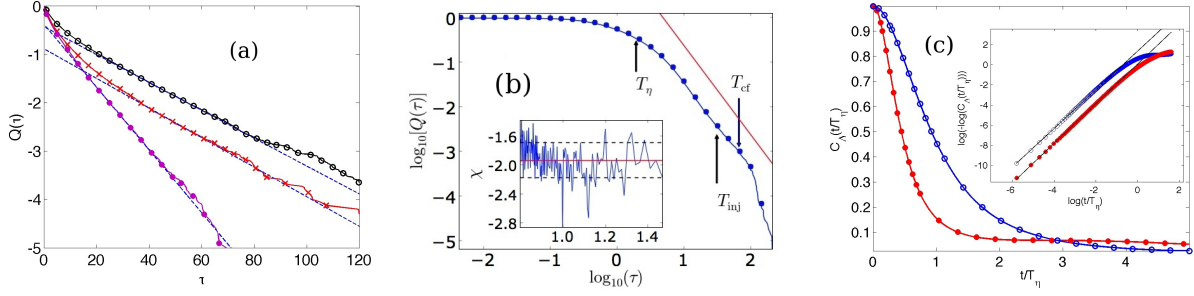


FIG. 2: (Color online) (a) Representative semilog plots (base 10) of the cumulative persistence-time PDFs  $Q_E^+$  (red crosses),  $Q_E^-$  (black open circles), and  $Q_L^-$  (magenta full circles); the subscripts  $E$  and  $L$  signify Eulerian and Lagrangian frames, respectively; and the superscripts  $+$  or  $-$  distinguish PDFs from vortical points from those from extensional ones. The dashed lines indicate exponential fits to these cumulative PDFs. These plots use data from our run R4. (b) A representative log-log plot (base 10) of the cumulative PDF  $Q_L^+(\tau)$  ( $\bullet$ ) versus  $\tau$  for our run R4; the full red line, with a slope equal to  $-2$ , is drawn for reference. The vertical arrows indicate the time scales (from left to right)  $T_\eta$ ,  $T_{\text{inj}}$ , and  $T_{\text{cf}}$ , respectively. The inset shows the local slope  $\chi = d\log_{10} Q_L^+(\tau)/d\log_{10}(\tau)$  versus  $\tau$ ; the horizontal line is drawn at the mean  $\langle \chi \rangle \simeq -1.93$  and the black dashed lines, drawn at  $\langle \chi \rangle \pm \sigma_\chi$ , where  $\sigma_\chi \simeq 0.2$  is the standard deviation of  $\chi$ . (c) Plots of the autocorrelation function of the Okubo-Weiss parameter  $C_A(t/T_\eta)$  (see text) versus  $t/T_\eta$  in Eulerian (blue open circles) and Lagrangian (red full circles) frames for our run R1. In the inset we compare the data points for these plots with their fits (full lines) to the form  $G \exp[-(t/T_A)^2]$ .

- Rev. Lett. **77**, 2867 (1996). B. Derrida, V. Hakim, and R. Zeitak, Phys. Rev. Lett. **77**, 2871 (1996).
- [3] M. Rivera, X. Wu, and C. Yeung, Phys. Rev. Lett. **87**, 044501 (2001).
- [4] P. Perlekar and R. Pandit, New J. Phys. **11**, 073003 (2009).
- [5] A. Okubo, Deep-Sea. Res. **17**, 445 (1970). J. Weiss, Physica (Amsterdam) **48D**, 273 (1991).
- [6] A. Perry and M. Chong, Annu. Rev. Flu. Mech. **19**, 125 (1987). P. Perlekar, PhD Thesis, Indian Institute of Science (2009; unpublished).
- [7] C. Canuto, M.Y. Hussaini, A. Quarteroni and T.A. Zang, Spectral methods in Fluid Dynamics (Springer-Verlag, Berlin, 1988).
- [8] S. M. Cox and P. C. Matthews, J. Comput. Phys. **176**, 430 (2002).
- [9] W. Press, B. Flannery, S. Teukolsky, and W. Vetterling, Numerical Recipes in Fortran (Cambridge University Press, Cambridge, 1992).
- [10] D. Mitra, J. Bec, R. Pandit, and U. Frisch, Phys. Rev. Lett **94**, 194501 (2005).
- [11] See, e.g., the supplementary material at <http://www.youtube.com/watch?v=ANDUNDHYgzk> for a movie generated from our DNS. This shows the time evolution of the vorticity field  $\omega$  and of a Lagrangian particle.
- [12] O. Cardoso, B. Gluckmann, O. Parcollet, and P. Tabeling, Physics of Fluids **8**, 209 (1996).
- [13] P. Beyer and S. Benkadda, Chaos **11**, 774 (2001).
- [14] B. J. Cantwell, Phys. Fluids A **5**, 2008 (1993).
- [15] H. Kallabis and J. Krug, Europhys. Lett. **45**, 20 (1999).